

## Encapsulation of OZ439 into Nanoparticles for Supersaturated Drug Release in Oral Malaria Therapy

Hoang D. Lu,<sup>†,§</sup> Kurt D. Ristroph,<sup>†,§</sup> Ellen L. K. Dobrijevic,<sup>†,§</sup> Jie Feng,<sup>†</sup> Simon A. McManus,<sup>†,§</sup> Yingyue Zhang,<sup>†</sup> William D. Mulhearn,<sup>†</sup> Hanu Ramachandruni,<sup>‡</sup> Anil Patel,<sup>‡</sup> and Robert K. Prud'homme<sup>\*,†</sup>

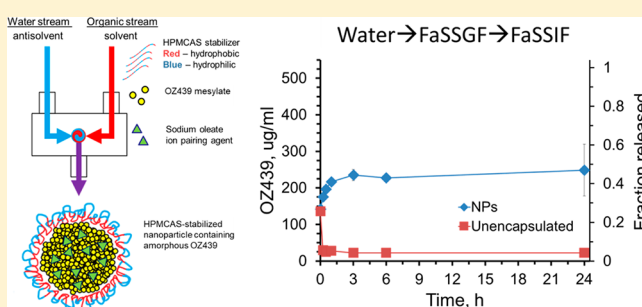
<sup>†</sup>Department of Chemical and Biological Engineering, Princeton University, A301 Engineering Quadrangle, Olden Street, Princeton, New Jersey 08542, United States

<sup>‡</sup>Medicines for Malaria Venture, Route de Pré-Bois 20, 1215 Meyrin, Switzerland

### Supporting Information

**ABSTRACT:** Malaria poses a major burden on human health and is becoming increasingly difficult to treat due to the development of antimalarial drug resistance. The resistance issue is further exacerbated by a lack of patient adherence to multi-day dosing regimens. This situation motivates the development of new antimalarial treatments that are less susceptible to the development of resistance. We have applied Flash NanoPrecipitation (FNP), a polymer-directed self-assembly process, to form stable, water-dispersible nanoparticles (NPs) of 50–400 nm in size containing OZ439, a poorly orally bioavailable but promising candidate for single-dose malaria treatment developed by Medicines for Malaria Venture (MMV). During the FNP process, a hydrophobic OZ439 oleate ion paired complex was formed and was encapsulated into NPs. Lyophilization conditions for the NP suspension were optimized to produce a dry powder. The *in vitro* release rates of OZ439 encapsulated in this powder were determined in biorelevant media and compared with the release rates of the unencapsulated drug. The OZ439 NPs exhibit a sustained release profile and several-fold higher release concentrations compared to that of the unencapsulated drug. In addition, XRD suggests the drug was stabilized into an amorphous form within the NPs, which may explain the improvement in dissolution kinetics. Formulating OZ439 into NPs in this way may be an important step toward developing a single-dose oral malaria therapeutic, and offers the possibility of reducing the amount of drug required per patient, lowering delivery costs, and improving dosing compliance.

**KEYWORDS:** nanocarrier, hydrophobic ion pairing, malaria, drug delivery, oral therapeutic



Malaria is an extremely prevalent infectious disease. The World Health Organization (WHO) estimates that in 2016, there were 212 million cases of malaria that resulted in 429,000 deaths worldwide.<sup>1</sup> sub-Saharan Africa and southeast Asia are particularly affected by malaria in terms of both health and economic burden, as they experience 90% and 7% of the global cases, respectively.<sup>1</sup> Furthermore, malaria is particularly lethal to children; 70% of malaria deaths were in children under five years old in 2015.<sup>1</sup>

Malaria is caused by several species of *Plasmodium* parasites: 99% of deaths are estimated to be from *Plasmodium falciparum*, and *Plasmodium vivax* is the next most prevalent strain.<sup>1,2</sup> Currently, WHO recommends treatment for uncomplicated cases of *P. falciparum* with an artemisinin-based combination therapy.<sup>1</sup> Artemisinin and its derivatives have a rapid onset of action and are highly potent, but have a short circulatory half-life of around half an hour after ingestion.<sup>4</sup> They are therefore paired with a longer acting partner drug, such as lumefantrine (half-life of 3–4 days) or piperaquine (half-life of 8–16 days).<sup>2</sup> The most common treatment schedule for adults is a three-day

regimen of 4 tablets a day.<sup>2,3</sup> The multi-day dosing regimen of these therapies poses a significant risk for resistance development, as patients often discontinue drug use before the end of the regimen in order to save medications for later use.<sup>5</sup> The development of a single-dose cure alleviates risks from resistance development due to patient non-adherence.<sup>2</sup>

Oral delivery is the preferred method of drug delivery for developing nations because of the easier administration, higher versatility, and lower manufacturing costs of oral therapeutics compared to injectable systems.<sup>6,7</sup> However, achieving drug delivery through the gastrointestinal (GI) tract can be impaired by unfavorable drug properties such as poor stability and low solubility in the GI tract, both of which result in low bioavailability.<sup>9</sup>

One way of improving the pharmacokinetics and therapeutic efficacy of existing orally administered drugs is through nanoparticle (NP) drug delivery systems, which may improve the dissolution kinetics and boost the solubility of an encapsulated

Received: December 25, 2017

Published: March 26, 2018

therapeutic.<sup>8,10–12,39</sup> In particular, polymeric NPs are commonly explored for the delivery of hydrophobic compounds. Polymeric NP properties such as size, surface composition, and charge can be chosen to improve a drug's dissolution kinetics, bioavailability, and pharmacokinetics, for example.<sup>12–14,29</sup>

Flash NanoPrecipitation (FNP) is an inexpensive and scalable method of producing polymeric NPs with tunable size and a narrow size distribution, as described previously.<sup>15</sup> In brief, an organic active and an amphiphilic polymer are dissolved in an organic solvent and are rapidly mixed with a miscible anti-solvent stream. A confined impinging jet (CIJ) mixer produces rapid mixing, creating supersaturation conditions that result in the precipitation of the hydrophobic active. The hydrophobic unit of the amphiphilic polymer is deposited on the surface of the organic active, allowing the outer hydrophilic block to sterically stabilize the NPs and preventing further growth and aggregation.<sup>15</sup> FNP can produce stable NPs containing hydrophobic organic actives at high loadings (>25%) and yields.<sup>16,17</sup> Importantly, FNP is a continuous process, which allows for scaling in time, and CIJs have been used in production of commercial products.<sup>15,18</sup> FNP has been used successfully to improve the oral dissolution kinetics of the hydrophobic drug clofazimine by encapsulating it into NPs via low-cost stabilizers.<sup>39</sup> The FNP process is therefore an appropriate platform for the large-scale production of therapeutics at low cost, which is required for the development of malaria treatments in developing countries.

OZ439, also known as artefenomel, is a synthetic peroxide antimalarial drug (Figure 1).<sup>19,20</sup> Preliminary studies indicate

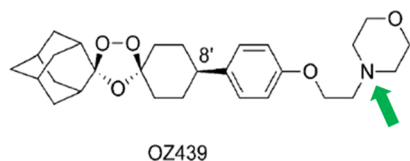


**Figure 1.** Structure of peroxide antimalarial drug OZ439 in its free base form.<sup>19</sup> The tertiary amine (arrow) is the site of our hydrophobic ion pairing.

that the efficacy of OZ439 is not affected by mutations known to cause resistance to artemisinin.<sup>20,23</sup> Like artemisinin, OZ439 has a fast onset of action; one important distinction is that OZ439's 25–30 h half-life is significantly longer than artemisinin's half-life of 0.5 h.<sup>19,21</sup> In a single oral dose of 20 mg/kg, OZ439 has proved curative in mice models infected with *P. berghei*. This result was superior to those obtained with all other tested synthetic peroxides and artemisinin derivatives, and could only be achieved by artemisinin with a partner drug.<sup>19</sup> Additionally, OZ439, when given as a single prophylactic dose of 30 mg/kg 48 h before infection, was preventative in mice and performed better than the same dose of mefloquine, the prophylactic drug currently used.<sup>19</sup> These results, as well as ease of synthesis, make OZ439 a promising candidate for a single-dose malaria cure.<sup>19,22</sup> The successful encapsulation of OZ439 into stable, water-dispersible NPs thus offers the possibility of improving oral bioavailability of this promising malarial therapeutic drug.

## EXPERIMENTAL SECTION

**Materials.** Affinisol HPMC-AS 126 G (>94% purity), Affinisol HPMC-AS 716 G (>94%), Affinisol HPMC-AS 912 G (>94% purity), and Methocel E3 Premium LV Hydroxypropyl Methylcellulose (HPMC E3) were purchased from Dow Chemicals. Poly(styrene)<sub>1.6kDa</sub>-*block*-poly(ethylene glycol)<sub>skDa</sub>

(PS-PEG) and polycaprolactone<sub>3.9 kDa</sub>-*block*-poly(ethylene glycol)<sub>skDa</sub> (PCL-PEG) were purchased from Polymer Source Inc. Vitamin E ( $\pm$ - $\alpha$ -tocopherol), Vitamin E succinate (D- $\alpha$ -tocopherol succinate), pamoic acid disodium salt (>97% purity), sodium deoxycholate (>97% purity), sodium dodecyl sulfate (>99% purity), sodium myristate (>98% purity), and sucrose BioXtra (>99.95% purity) were purchased from Sigma-Aldrich. Tetrahydrofuran (HPLC grade, 99.9%), methanol (HPLC grade, 99.9% purity), and acetone (HPLC grade, 99.9% purity) were purchased from Fisher Chemicals. Sodium oleate (>97% purity) was purchased from TCI America. Phosphate buffered saline 10X (PBS) without calcium or magnesium was purchased from Lonza.<sup>28</sup> Fasted-state simulated intestinal fluid (FaSSIF), fed-state simulated intestinal fluid (FeSSIF), and fasted-state simulated gastric fluid (FaSSGF) were purchased from biorelevant.com.<sup>27</sup> Mannitol (>96.0% purity) from BDH was purchased from VWR. OZ439 mesylate was supplied by Medicines for Malaria Venture (MMV).

**Hydrophobic Ion Pairing Screen.** Artefenomel mesylate (henceforth referred to as OZ439) is a moderately hydrophobic compound ( $\log P = 4.6$ ) that, after being dissolved in organic solvents (THF or 33% methanol and 67% THF), does not precipitate into stable NPs through the FNP process.<sup>36</sup> Instead, OZ439 rapidly crystallizes and produces macroscopic precipitates after FNP when processed without any additional excipients or polymeric stabilizers.

To assess if OZ439 could be converted into a hydrophobic ion paired complex, five anionic species were considered as candidates for hydrophobic ion pairing: sodium oleate (OA), pamoic acid disodium salt, sodium deoxycholate, sodium dodecyl sulfate (SDS), and sodium myristate (Figure 2). These candidates

	<b>Sodium Oleate</b> MW: 304.44 g/mol pKa: 5.0 clogP: 7.58
	<b>Pamoic Acid Disodium Salt</b> MW: 432.3 g/mol pKa: 2.7 clogP: 5.52
	<b>Sodium deoxycholate</b> MW: 414.6 g/mol pKa: 4.65 clogP: 4.25
	<b>Sodium dodecyl sulfate (SDS)</b> MW: 288.4 g/mol pKa: -1.5 clogP: 2.83
	<b>Sodium myristate</b> MW: 250.2 g/mol pKa: 5.0 clogP: 6.05

**Figure 2.** Candidates for hydrophobic ion pairing with OZ439.

were chosen since they all possess an anionic ionizable group and a hydrophobic functional group.<sup>40</sup> The anions interact with the cationic group on OZ439 in solution, resulting in the formation of a hydrophobic ion paired complex.<sup>24</sup> [Note: The term “hydrophobic ion paired complex” is used herein to denote the construct formed during this counterion exchange; the term is somewhat interchangeable with “salt”, but “salt” is usually reserved for crystalline materials with strictly defined stoichiometric ratios of anions and cations. Our ultimate formulation employs an excess of the hydrophobic anion, so while the cationic moieties on OZ439 are complexed with opposite anionic

moieties on the anion, there may be some excess free anion in the hydrophobic complex, and the precipitate is not crystalline.]

OZ439 mesylate salt was dissolved with an ion pair candidate at varying charge ratios in organic solvents. The organic solution was then diluted 2-fold with water to mimic the anti-solvent stream in the FNP process, and the presence, speed, and amount of precipitation were observed. Additional water was then added for a final ratio of organic to water of 1:10 to determine if precipitation of the hydrophobic species would occur upon the dilution of the organic phase in the final step of FNP. The formation of a precipitate indicated the formation of a hydrophobic ion paired complex.

**OZ439 Conversion into Free Base Form.** In order to improve hydrophilicity, OZ439 is manufactured as a mesylate salt form, with its tertiary amine protonated. Studies have shown that in simulated gastric fluid, regardless of the initial salt pair, OZ439 forms a very poorly soluble hydrochloride salt.<sup>19</sup> The uncharged free base form of OZ439 (OZ FB) has not been tested *in vivo*; if OZ439 can be stabilized as a free base *in vivo*, conversion to the poorly soluble hydrochloride salt form may be prevented. Therefore, OZ FB was also considered for encapsulation in NPs.

OZ FB was created by exchange in basic water. In brief, OZ439 mesylate was dissolved in methanol at 20 mg/mL. A 10-fold volume of 1 M NaOH was added to OZ439 dissolved in methanol. The precipitated OZ439 base was isolated by centrifugation at 10000g for 10 min, and the supernatant was removed. OZ439 free base was rinsed by re-suspension in equivalent volume of water and isolated by centrifugation at 10000g for 10 min. Remaining moisture in the drug was removed by placing the compound at <20 Torr pressure overnight.

**OZ439 Mesylate and OZ Free Base Complexation into Nanoparticles.** NPs were made through Flash Nano-Precipitation (FNP) using a confined impinging jet (CIJ) mixer. The organic actives, stabilizers, and ion pairs or co-cores were dissolved in organic solvents (either acetone or a mixture of 33% methanol and 67% THF, depending on the solubility of the relevant species). The final concentrations of the active and stabilizer in the solution were each 5 mg/mL unless otherwise noted. The solution was then sonicated to ensure complete mixing and dissolution. Equal volumes (0.5 mL) of the organic solution and water anti-solvent were placed in separate syringes and attached to the CIJ mixer. The organic stream and anti-solvent stream were simultaneously and rapidly ejected from the syringes through the CIJ mixer. The resultant combined stream containing NPs was collected in a vial containing 4 mL of water (thus, each feed stream was diluted 10-fold, and the final solution contained 90% water and 10% organic solvents).

**Nanoparticle Characterization.** NP size and stability were assessed using dynamic light scattering (DLS; Malvern Zetasizer Nano, Malvern Instruments to determine average size, size distribution, and polydispersity index (PDI), at 0, 1, 3, 6, and 24 h time points following FNP.<sup>26,33,34</sup> Samples were diluted 10-fold prior to DLS to avoid multiple scattering. The size is determined from the first cumulant of the series expansion of the light scattering correlation function. The PDI is obtained from the Taylor series expansion of the autocorrelation function, and is incorporated into the Malvern Nanosizer data analysis software. A ratio of one-half of the second moment to the first moment is defined as the PDI, where values of 0.1 are generally obtained for monodisperse particles.<sup>37,38</sup>

Zeta potential measurements were also measured using the Malvern Zetasizer Nano-ZS. The samples were diluted 10-fold

into 0.1X PBS in a disposable folded capillary cell (DTS1070) and measured.

**Nanoparticle Processing into Powder Form.** NP suspensions containing therapeutics must be processed into dry powders for transportation and long-term storage. Ideal powders are those which can re-disperse easily in water and preserve the original NPs' properties such as size and size distribution. Promising formulations were selected for processing into dry powders by lyophilization. Prior to lyophilization, NP solutions were stabilized against aggregation during freezing through the addition of a cryoprotectant. The identity and amount of the cryoprotectant added to the NP solution were varied.

NP suspensions with added cryoprotectants were quickly frozen in an acetone bath cooled to  $-78\text{ }^{\circ}\text{C}$  by dry ice. For lyophilization, flash-frozen samples were transferred to a  $-80\text{ }^{\circ}\text{C}$  freezer to ensure complete freezing.<sup>31</sup> A VirTis AdVantage freeze-dryer at  $-20\text{ }^{\circ}\text{C}$  and under vacuum was used to remove the water and organic solvents from the NPs, forming a dry powder of the NP sample.

**Drug State.** X-ray diffraction patterns were collected in reflection using a Philips-Norelco wide-range goniometer and scintillation counter, equipped with an Advanced Materials Research graphite focusing monochromator. Cu  $K\alpha$  radiation ( $\lambda = 0.15418\text{ nm}$ ) was produced via a PANalytical PW3830 X-ray generator with a long-fine-focus Cu tube. Angular calibrations were performed using a quartz reference standard. Samples were deposited as a loose powder ( $\sim 0.5\text{ mm}$  deep) onto carbon tape, supported on a glass microscope slide. Sample crystallinity was assessed by the presence or absence of strong Bragg reflections.<sup>35</sup>

**Nanoparticle Release.** The *in vitro* release of the active OZ439 from NPs over time in simulated biorelevant media was determined and compared to the release of the active from the unprocessed active in powder form. To measure OZ439 dissolution kinetics in biorelevant media, NPs or un-encapsulated free powder was suspended in water or different media and incubated at  $37\text{ }^{\circ}\text{C}$  in a water bath. In some cases, as described in the Results and Discussion section, a "media swap" from water, through gastric fluid, into intestinal fluid was performed. At 0, 0.25, 0.5, 1, 3, 6, and 24 h, the concentration of the organic active in solution was measured. An aliquot was removed from the solution and spun in an Eppendorf 5430R centrifuge at 21000 g for 15 min in order to pellet any NPs present. The supernatant was then removed and lyophilized. The resulting powder was resuspended in a solution of 10% THF and 90% acetonitrile in order to dissolve any OZ439. The aliquot was again centrifuged for 15 min to pellet insoluble bile salts and cryoprotectants. The supernatant was then removed, filtered through a GE Healthcare Life Sciences Whatman 0.1  $\mu\text{m}$  syringe filter, and analyzed by high-performance liquid chromatography (HPLC) to determine the concentration of the organic active. The HPLC was operated at  $45\text{ }^{\circ}\text{C}$ , with an isocratic mobile phase of 100% acetonitrile with a Gemini C18 column (particle size 5  $\mu\text{m}$ , pore size 110  $\text{\AA}$ ) and a 6.5 min run time. The UV detector took measurements at 200, 220, and 276 nm. Measurements were performed in triplicate.

## RESULTS AND DISCUSSION

**Hydrophobic Ion Pairing Screening.** When diluted 2-fold in water, OZ439 with SDS, pamoic acid disodium salt, and sodium deoxycholate did not form stable precipitates; either no reaction was visible, or a precipitate formed on initial mixing but quickly re-dissolved (Table 1). When diluted 10-fold in water,

**Table 1. Results of Precipitation Test for OZ439 Ion Pair Candidates<sup>a</sup>**

IP	ratio of OZ439:IP	precipitation in 1:1 organic:water	precipitation in 1:10 organic:water
none	1:0	—	—
sodium oleate (OA)	0:1	—	—
	1:1	+	+
	1:2	+	+
	1:3	+	+
	1:4	—	—
pamoic acid	0:1	—	—
	1:1	*	+
	1:2	*	+
	1:3	*	+
	1:4	*	+
sodium deoxycholate	0:1	—	—
	1:1	—	+
	1:2	—	+
	1:3	*	+
	1:4	*	+
SDS	0:1	—	—
	1:1	—	+
	1:2	—	—
	1:3	—	*
	1:4	—	*

<sup>a</sup>Key: —, no precipitation observed; +, immediate precipitation observed; \*, precipitate formed initially but quickly redissolved.

OZ439 with pamoic acid disodium salt and sodium deoxycholate did form stable precipitates. OZ439 with oleic acid (OA) formed a precipitate immediately upon 2-fold dilution, as well as upon 10-fold dilution with water. OZ439 with OA in a molar ratio of 1:1 formed the most precipitate and most rapidly, compared to other ion pairs at a 1:1 OVA:IP ratio. These results have identified OA as a promising ion pair for converting OZ439 into a hydrophobic ion paired complex for use in FNP.

**OZ439 Complexation into Nanoparticles and NP Characterization.** OZ439 Mesylate. FNP was used to produce NPs comprising OZ439, a stabilizing polymer, and an ion pair or co-core. The ratio of OZ439 to the ion pair or co-core and the identity of the stabilizing polymer were varied.

When subjected to FNP, OZ439 mesylate without stabilizer formed large aggregates (Figure S1B). OZ439 mesylate and OA ion pair formed NPs without a stabilizing polymer (Figure S1); however, these NPs were unstable, and crystals formed after 3–6 h. Additional characterization data on these NPs is found in the SI.

To formulate sterically stabilized NPs, OZ439:OA was subjected to FNP processing using the HPMC-AS 126, HPMC-AS 716, and HPMC-AS 912, as well as the polycaprolactone-*block*-polyethylene glycol (PCL-*b*-PEG). PCL-*b*-PEG is an amphiphilic block copolymer, and the HPMC-AS grades are cellulosic polymers with acetyl and succinyl substitutions. HPMC-AS 716 has the highest degree of succinyl substitutions, making it the most negatively charged, while HPMC-AS 126 has the most acetyl substitutions and is the most hydrophobic.<sup>30</sup> These stabilizers were used to make NPs with molar ratios of OZ439:OA of 1:1, 1:2, and 1:4 (Figure 3). None of the formulations tested with PCL-*b*-PEG were stable. Apparently, both the hydrophobic

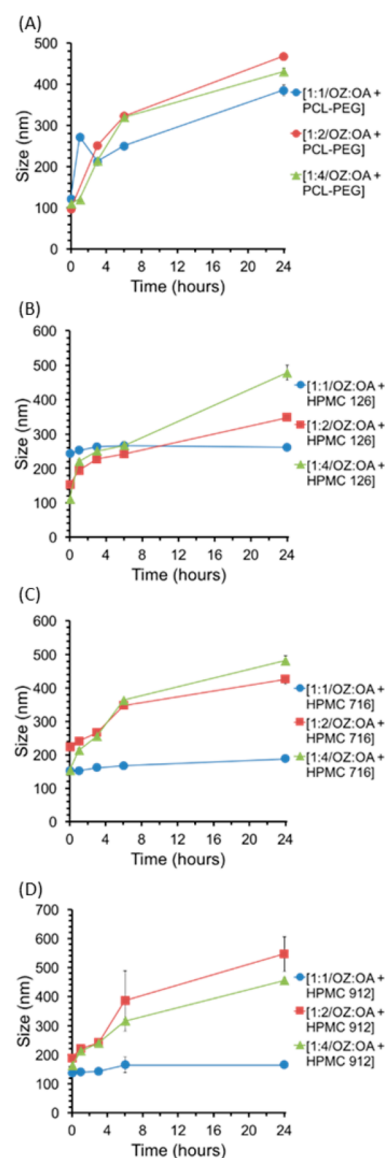


**Figure 3.** Nanoparticles with ratios of OZ439:OA of 1:1, 1:2, and 1:4 with stabilizers PCL-PEG (A), HPMC-AS 126 (B), HPMC-AS 716 (C), and HPMC-AS 912 (D). The average size over time are shown to compare stability of formulations. PCL-PEG stabilized NPs increased in size significantly over time (A). For each HPMC stabilizer 1:1 OZ439 to OA was the most stable, all remained within 25% of their initial average size. NPs with HPMC-AS 126 or 716 maintained a narrow size distribution over 24 h (B,C). NPs made with HPMC-AS 912 the PDI reached a maximum of  $0.26 \pm 0.07$ ,  $0.39 \pm 0.21$ , and  $0.15 \pm 0.04$  for 1:1, 1:2, and 1:4 OZ439 to OA, respectively. The most promising formulations were 1:1 OZ439:OA with either HPMC-AS 126 or HPMC-AS 716 as a stabilizer, increasing in average size by only 9% and 24%, respectively (B,C). For PDI information, see Figure S3.

interactions and the ionic interactions (succinate groups on HPMC-AS) are required for stability. The HPMC-AS 126, HPMC-AS 716, and HPMC-AS 912 stabilizers at a ratio of 1:1 OZ439:OA yielded the most stable particles, with an average size increase of 9% (20 nm), 24% (38 nm), and 21% (23 nm) over 24 h, respectively (Figure 3). HPMC-AS 126 and 716 produced NPs that were roughly comparable with respect to size stability and PDI for molar ratios of OZ439:OA of 1:1. HPMC-AS 126 demonstrated greater stability with a OZ439:OA ratio of 1:2 than HPMC-AS 716, especially over the first 6 h

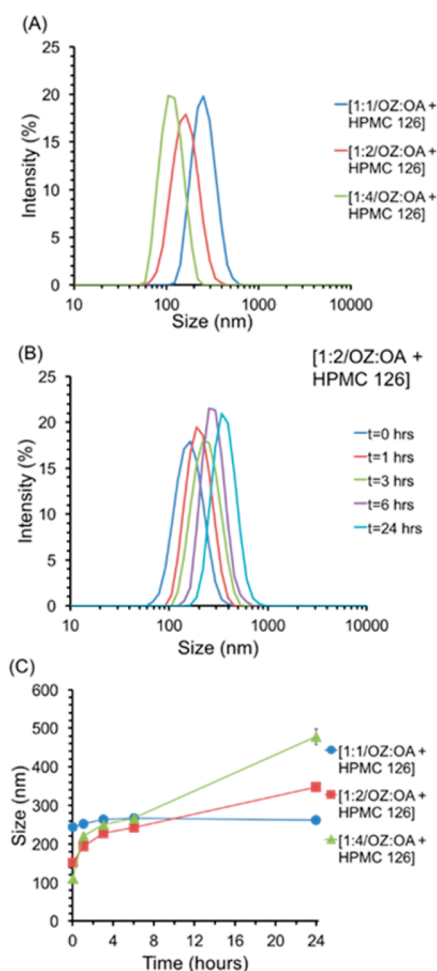


**Figure 4.** Nanoparticle formulations with molar ratios of OZ439:OA of 1:1, 1:2, and 1:4 with the polymer HPMC-AS 126, comparison of initial size distribution (A), average size (C) over time for 24 h. Increasing the molar ratio of OZ439 to OA decreased the size of the NPs; this could be a result of increased nucleation (A). The average size of the NPs increased by  $23 \pm 18$  nm,  $90 \pm 7$  nm, and  $156 \pm 5$  nm over 6 h for OZ439:OA ratios of 1:1, 1:2, and 1:4, respectively (C). The molar ratio of OZ439:OA of 1:1 with HPMC-AS 126 produced the most stable NPs. The size distribution over time of 1:2 OZ439 to OA NPs showed that although the size increased over 24 h from an average size of  $152 \pm 3$  nm to  $348 \pm 2$  nm no aggregates above 1000 nm appeared (B).

(Figures 3 and 4). Therefore, HPMC-AS 126 with molar ratios of 1:1 or 1:2 of OZ439:OA or HPMC-AS 716 with a molar ratio of 1:1 OZ439:OA were the most promising formulations.

Ion pairing of a hydrophobic salt, and organic active can be performed *in situ*, as in the above experiments, or prior to the FNP process. Pre-ion paired constructs were produced by precipitation with OZ439:OA molar ratios of 1:1, and 1:2, and by precipitation with ratios of 1:1, 1:2, and 1:3. The initial size distribution, and trends in size over time for NPs with 1:2 OZ439:OA were similar regardless of ion pairing method or stabilizer (Figure 5). NPs with pre-ion-paired 1:1 OZ439:OA were less stable than *in situ* ion paired NPs (Figure 5).

**OZ439 Free Base.** OZ FB alone did not form NPs with stabilizers HPMC-AS 126, HPMC-AS 716, and HPMC-AS 912 without ion pairing. When supplemented with VitE-S at a 1:2 molar ratio of OZ FB to VitE-S, the free base form of the drug could be made into stable NPs with each of the three

HPMC-AS polymers. In this case, the anionic succinate group acts as the ion pairing agent. HPMC-AS 126 and HPMC-AS 716 were selected to investigate the effect of changing the molar ratios of OZ FB to VitE-S (Figures 6 and 7). NPs were made with a ratio of 1:1, 1:2, and 1:4 OZ FB:VitE-S and stabilized by either of these two HPMC-AS polymers.

**Nanoparticle Processing into Powder Form.** OZ439 NPs with a molar ratio of OZ439:OA of 1:2 with the stabilizer HPMC-AS 126 were lyophilized. This formulation was selected because it was stable enough to allow for processing and displayed consistent properties when formed by *in situ* ion pairing and pre-ion pairing. Three cryoprotectants were considered—sucrose, mannitol, and HPMC E3—and mass ratios of NPs to cryoprotectant of 1:0, 1:0.5, 1:1, 1:3, and 1:10 were tested to determine the most effective species of cryoprotectant and the minimum amount required. To investigate the effects of freezing on the NPs' properties, each sample tested for lyophilization was also frozen and then thawed, and the NP characteristics were analyzed using DLS. All samples tested, including those without any cryoprotectant, re-dispersed readily upon thawing. After lyophilization, NPs with a 1:2 ratio of OZ439:OA with HPMC-AS 126 coatings with all ratios of sucrose, mannitol, and HPMC E3 as well as with no added cryoprotectant re-dispersed readily in water. For mass ratios greater or equal to 1:1, the average size of the re-dispersed NPs was under 250 nm for all tested cryoprotectants (initial NPs were 150 nm) (Figure 8). The dry powder formulation of 1:2 OZ439 to OA NPs with HPMC-AS 126 and the cryoprotectant HPMC E3, added in a mass of NPs to cryoprotectant ratio of 1:1, was selected as the optimized formulation to use in *in vitro* release rate studies.

OZ439 free base NPs, when lyophilized, did not form a powder that could re-disperse back to the nanoscale, as the OZ439:oleate NPs did. This failure to re-disperse would likely result in reduction of OZ439 dissolution kinetics, so the free base formulation was not pursued into the *in vitro* release stage.

**Drug State.** Powder X-ray diffraction was performed to identify whether the samples were crystalline, as identified by the presence of Bragg's peaks, or amorphous. Samples of the components of each NP formulation as well as the dried NPs were prepared, and XRD measurements were performed.

Both OZ439 mesylate and OZ439 free base are crystalline and have distinct Bragg peaks (Figure 9). In an amorphous drug state, the amorphous solid's energy state is higher than that of a crystal lattice, and the compound's dissolution kinetics are enhanced.<sup>25</sup> The XRD results indicate that the NPs are substantially amorphous, as the signals from both NP formulations are broad peaks (Figure 10).

**Nanoparticle Release.** The release of OZ439 from the chosen lyophilized NP powder—1:2 OZ439:OA, stabilized with HPMC-AS 126 and cryoprotected at a mass ratio of 1:1 with HPMC E3—was compared to the release from un-encapsulated OZ439 mesylate powder.

To mimic oral administration and *in vivo* conditions as accurately as possible, release experiments were carried out at  $528 \mu\text{g/mL}$  and involved a "media swap". For children, it is anticipated that an OZ439 NP powder would be dispersed in water and administered orally as a suspension. To imitate these conditions of administration *in vitro*, OZ439 NPs or un-encapsulated powder was dispersed in water, FaSSGF was then added, and the solution was incubated for 15 min, the average duration of substances in the stomach of a fasted subject.<sup>32</sup> The solution was then diluted in either FeSSIF or FaSSIF and incubated at  $37^\circ\text{C}$ , and the concentration of

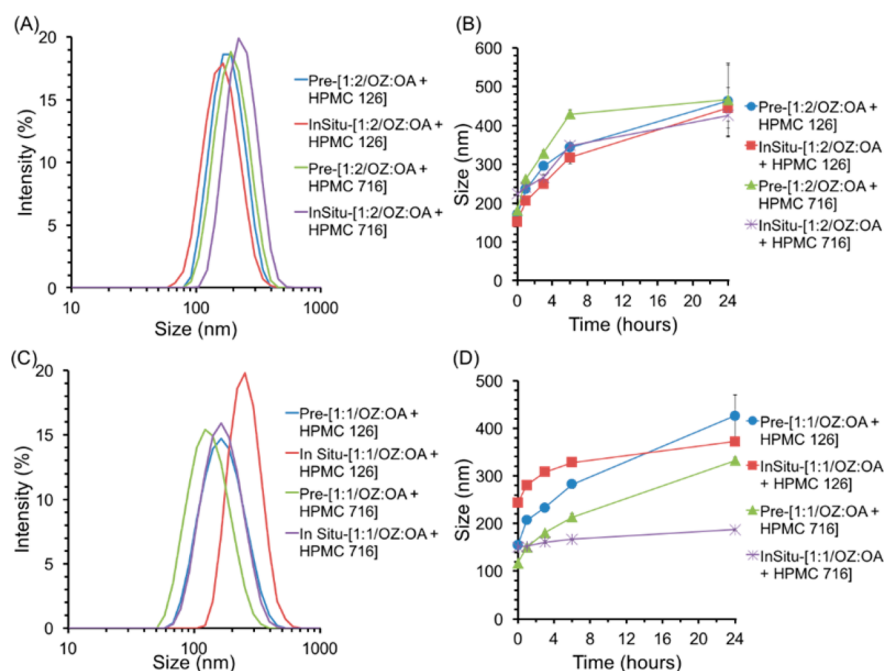


**Figure 5.** Comparison of nanoparticles formed with pre-ion paired or *in situ* ion paired OZ439, and OA, with stabilizing polymers of either HPMC-AS 126 or HPMC-AS 716. NPs with molar ratios of OZ439:OA of 1:2 initially formed NPs with average sizes between 150, and 240 nm (A). Furthermore, the size over time were similar for all NPs with 1:2 OZ439 to OA, with either HPMC-AS 126 or HPMC-AS 716, and either ion paired *in situ* or pre-ion paired by precipitation (B). On the other hand, there were more significant differences between the NP behaviors formed by ion pairing *in situ* or by precipitation for OZ439 to OA ratios of 1:1 for both HPMC-AS 126 and HPMC-AS 716 (C,D). Furthermore, the pre-ion paired NPs increased in average size more than *in situ* ion paired NPs (D). NPs with molar ratios of OZ439:OA of 1:2 demonstrated less variation in initial average size and more similar trends in size over time regardless of variations in ion pairing method or block copolymer. This suggested that particles formed with OZ439 to OA ratios of 1:2—that is, with excess ion pair with respect to OZ439—were less influenced by processing conditions, and might demonstrate greater stability.

OZ439 in solution was then measured at 0, 0.25, 0.5, 1, 3, 6, and 24 h.

In FaSSIF, the NPs achieved OZ439 concentrations up to 11 times higher than that of the un-encapsulated powder (Figure 11A). The maximum concentration of OZ439 released from the NPs was 248  $\mu\text{g}/\text{mL}$  at 1 h and from the un-encapsulated powder was 136  $\mu\text{g}/\text{mL}$  after 15 min. Notably, the concentration of OZ439 in solution released from NPs was always higher than that of the maximum concentration achieved by the un-encapsulated powder. Therefore, the NPs were effective in increasing the dissolution of OZ439 over an extended period. The un-encapsulated active demonstrated an early maximum concentration of OZ439 in solution followed by a decline in concentration, possibly due to recrystallization of OZ439 in solution.<sup>25</sup>

In FeSSIF, the maximum concentration of OZ439 from the NPs was 400  $\mu\text{g}/\text{mL}$  at 24 h, and from the unencapsulated powder was 380  $\mu\text{g}/\text{mL}$  at 30 min (Figure 11B). These preliminary experiments demonstrate that OZ439 NPs improve the solubility and sustained release of OZ439 compared to that in the un-encapsulated powder in FaSSIF. Since malaria patients often have little to no appetite, inducing a fed state is difficult. Thus, the ability to achieve rapid OZ439 dissolution in the fasted state, shown here using NPs, may help to ease drug administration without sacrificing efficacy.

Additional release experiments not involving the media swap were carried out in water, simulated gastric (FaSSGF), fasted-state simulated intestinal (FaSSIF), or fed-state intestinal (FeSSIF) fluid, into which lyophilized NPs or OZ439 mesylate powder was suspended to an OZ439 concentration of 140  $\mu\text{g}/\text{mL}$

and incubated in a water bath at 37 °C. Figure S8 contains the results of these more rudimentary release experiments.

In summary, OZ439 could be encapsulated in a stable NP formulation comprising OZ439 in a molar ratio to OA of 1:2 and the polymer stabilizer HPMC-AS 126. OZ439 NPs with a 1:2 molar ratio to OA and HPMC-AS 126 could be successfully lyophilized with the addition of HPMC E3 in a mass ratio of NPs to cryoprotectant of 1:1, with an overall drug loading of 16% in the final powder. Lyophilization produced powders that were easily re-dispersed in water with a narrow size distribution and average size of  $227 \pm 17$  nm. Furthermore, during *in vitro* release studies, these NPs demonstrated improved dissolution levels and sustained release several-fold higher than that of the un-encapsulated OZ439 powder when swapped from water into simulated fasted-state simulated intestinal fluid via simulated gastric fluid.

## CONCLUSION

The work presented demonstrates that OZ439, a synthetic antimalarial that has demonstrated safety and efficacy in human trials, can be encapsulated into polymer-stabilized nanoparticles to potentially improve its oral bioavailability. Improving the bioavailability of OZ439 could be a step toward developing a single dose cure for malaria, which could eliminate concerns of patient adherence and enhance efforts for malaria eradication. The cheap and scalable FNP process was used to formulate OZ439 into polymer-stabilized NPs, using FDA-approved and inexpensive excipients. Two forms of the active were used: OZ439 mesylate and OZ439 free base. Though OZ439 free base could be made into stable NPs, it could not be successfully

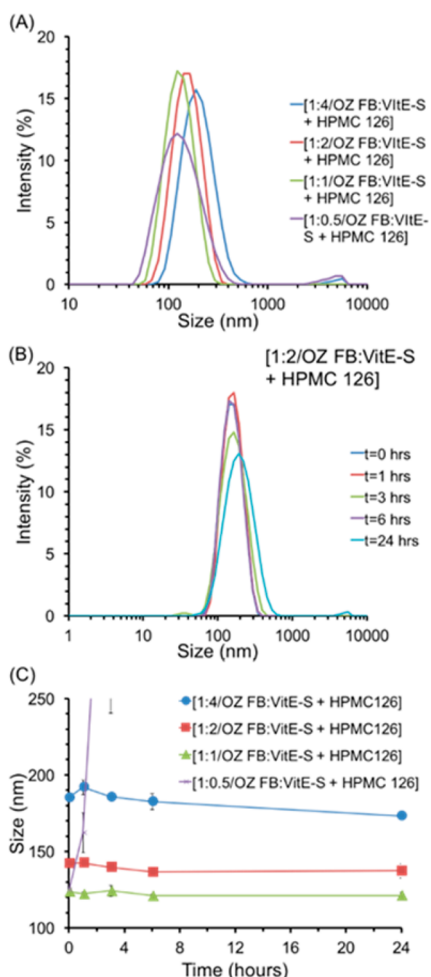


**Figure 6.** Effect on nanoparticle stability of changing the ratio of OZ FB to VitE-S, with HPMC-AS 126. The initial size distribution of each formulation tested, with ratios of OZ FB to VitE-S of 1:0.5, 1:1, 1:2, and 1:4 demonstrate that increasing concentrations of VitE-S led to larger NPs (A). The size distribution over time for NPs with 1:2 OZ FB to VitE-S and HPMC-AS 126 shows the stability of the NPs: at 24 h there was a small fraction of NPs greater than 1000 nm (B). The average size over time demonstrates the increase in size with increasing concentrations of VitE-S, as well as the stability of NPs with OZ FB to VitE-S ratios of 1:1, 1:2, and 1:4 (C). Together these figures demonstrate that OZ FB to VitE-S ratios of 1:1, 1:2, and 1:4 produced stable NPs, while a ratio of 1:0.5 did not produce stable NPs. For PDI information, see [Figure S5](#).

processed into dry powder form via lyophilization and was not investigated further.

It was shown that OZ439 mesylate could be successfully complexed with sodium oleate to form a hydrophobic ion pair. This complex forms stable NPs through FNP, unlike the weakly hydrophobic OZ439 mesylate. The stability of NP formulations of OZ439 with varying molar ratios to sodium oleate and different polymer stabilizers was analyzed. NPs of OZ439 with a molar ratio to OA of 1:2 and with the polymer stabilizer HPMC-AS 126 were found to be stable in solution and could be lyophilized with the addition of HPMC E3, producing a powder that re-dispersed readily in water with largely unmodified NP properties compared to the unprocessed NPs and with an overall drug loading of 16%.

The *in vitro* release rates of OZ439 from NPs and the un-encapsulated active were analyzed via a media swap experiment

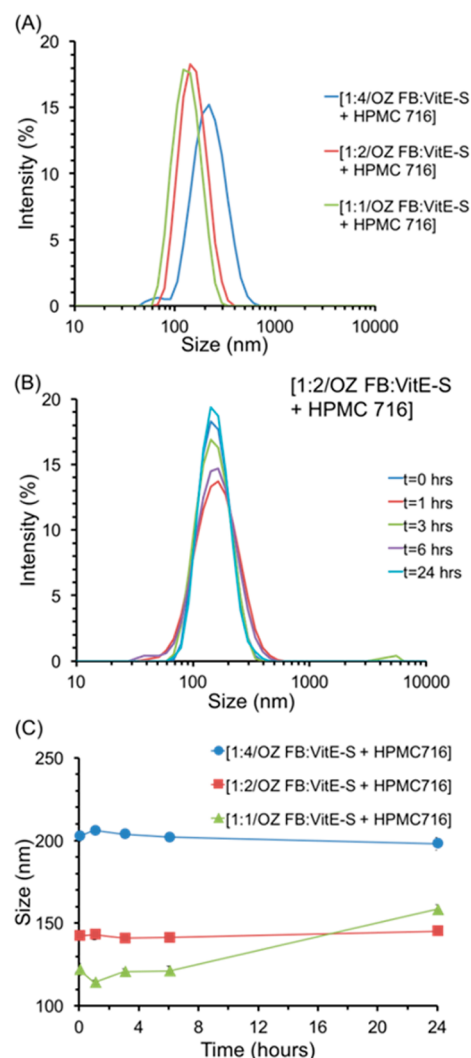


**Figure 7.** OZ FB nanoparticles with HPMC-AS 716 and varying molar ratios of OZ FB to VitE-S. The initial size distribution of each formulation tested, with ratios of OZ FB to VitE-S of 1:1, 1:2, and 1:4 demonstrates that increasing concentrations of VitE-S led to larger NPs (A). The size distribution over time for NPs with 1:2 OZ FB to VitE-S and HPMC-AS 126 shows the stability of the NPs; at 3 h, there was a small fraction of NPs greater than 1000 nm (B). The average size over time demonstrates the increase in size with increasing concentrations of VitE-S, as well as the stability of NPs with OZ FB to VitE-S ratios of 1:2 and 1:4 (C). NPs with OZ FB to VitE-S ratio of 1:1 were stable for the first 6 h, but there was a moderate increase in size at 24 h (C). For PDI information, see [Figure S6](#).

analogous to oral administration. When swapped from water through simulated gastric fluid to fasted-state simulated intestinal fluid, superior OZ439 release from NPs, including sustained supersaturation, was observed. In these conditions, the concentration of OZ439 released from NPs was up to 11-fold higher than that in the unencapsulated powder. Our results indicated that OZ439 NPs could demonstrate increased dissolution and bioavailability compared to that of the unprocessed OZ439 mesylate.

The most significant limitation of this approach is the expense of lyophilization. As emphasized by the OZ439 free base example, dry powder processing is an essential keystone in the formulation of a therapeutic for the developing world, as dry powders are less heavy (i.e., easier to ship) and likely more stable than liquid formulations. Since dry powder processing is required to be industrially relevant, alternatives to expensive lyophilization—for

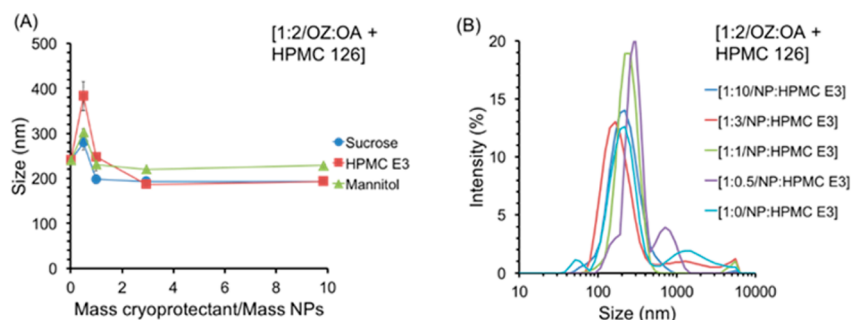


**Figure 8.** Effect of species and amount of cryoprotectant on average size (A) of redispersed lyophilized powder of 1:2 OZ439 to OA nanoparticles with the stabilizer HPMC-AS 126. HPMC E3 was the most promising cryoprotectant; the size distribution (B) of the redispersed powders with varying mass ratios of NP to HPMC E3 is shown. For NP:cryoprotectant mass ratios above 1:1 the average size of the redispersed NPs was relatively constant, at  $195 \pm 2$  nm,  $209 \pm 28$  nm, and  $227 \pm 5$  nm for sucrose, HPMC E3, and mannitol, respectively (A). Increasing the amount of HPMC E3 cryoprotectant generally reduced the level of aggregates present on redispersion, there was only a small tail of aggregates present in the size distribution at 1:1, 1:3, and 1:10 mass of NPs to HPMC E3 (B). For PDI and correlogram information, see Figure S7.

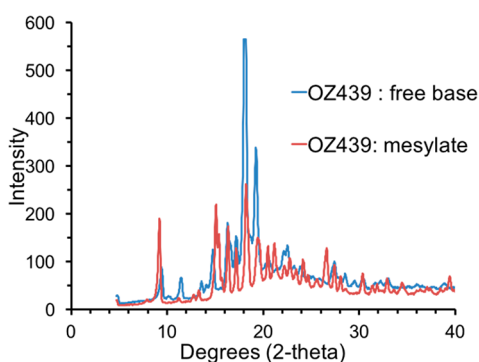


**Figure 9.** XRD results from OZ439 free base and OZ439 mesylate powders. The distinct Bragg peaks of each sample indicate they were distinct crystalline powders.

example, spray-drying—should be considered in future studies of this process. The stability of dry powders produced via these unit operations should also be examined in hot and humid conditions. Other immediate future work includes further release rate studies, long-term stability characterization, exploring additional powder processing routes such as spray drying, bioavailability studies, and animal toxicology studies.

## ■ ASSOCIATED CONTENT

### Supporting Information

The Supporting Information is available free of charge on the ACS Publications website at DOI: [10.1021/acsinfectdis.7b00278](https://doi.org/10.1021/acsinfectdis.7b00278).

Size information over time for NPs formed at different OZ439:OA or OZ439FB:VitE-S ratios; size profiles over time for OZ439 NP formulations with different stabilizers

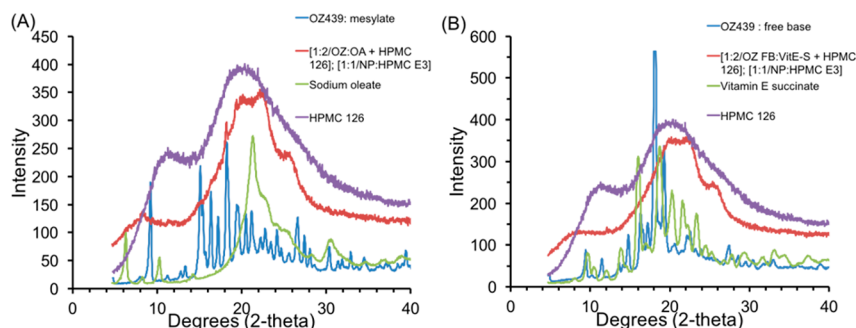


**Figure 10.** XRD results for OZ439 mesylate NPs (A) and OZ439 free base NPs (B).

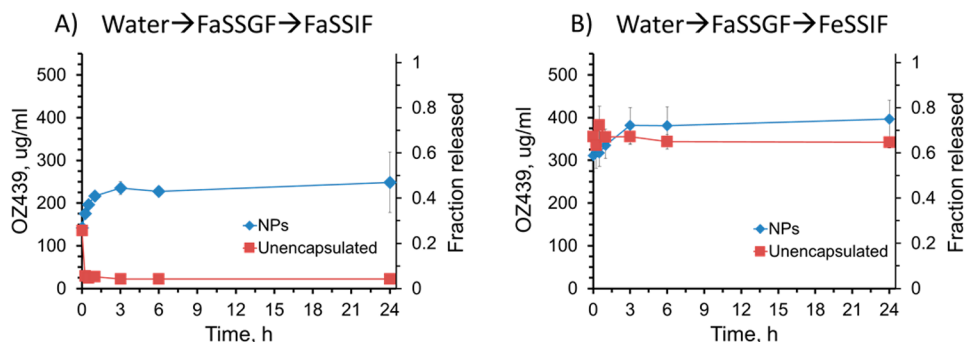


**Figure 11.** Release of OZ439 from nanoparticles and unencapsulated powder after media swap experiment. The samples were first dispersed in water, then FaSSGF, then into either FaSSIF (A) or FeSSIF (B). In FaSSIF the concentration of OZ439 was on average 7.8-fold higher from NPs compared to the unencapsulated powder (A). The powder's early maximum in concentration indicated an initial burst release followed by recrystallization.



in different media; correlograms and size profiles detailing the effect of differing NP: cryoprotectant mass ratios; OZ439:OA NP *in vitro* release when diluted directly into various biomedica (instead of the more realistic media swap release) at 140  $\mu\text{g}/\text{mL}$ ; and differential scanning calorimetry on the hydrophobic ion paired complex of OZ439 cation and oleate anion, including Figures S1–S9 (PDF)

## AUTHOR INFORMATION

### Corresponding Author

\*E-mail: [prudhomme@princeton.edu](mailto:prudhomme@princeton.edu).

### ORCID

Simon A. McManus: 0000-0003-1714-1259

### Author Contributions

<sup>§</sup>H.D.L., K.D.R., and E.L.K.D. are co-first authors.

### Notes

The authors declare no competing financial interest.

## ACKNOWLEDGMENTS

The work was supported by the Bill and Melinda Gates Foundation (OPP1150755). The authors thank Dr. Pius Tse, Dr. Chih-Duen Tse, Dr. Niya Bowers, and Dr. Ben Boyd for intellectual discussions. This material is based upon work supported by the National Science Foundation Graduate Research Fellowship under Grant No. DGE-1656466 awarded to K.D.R.

## ABBREVIATIONS

CIJ, confined impinging jet; DLS, dynamic light scattering; FaSSIF, fasted-state simulated intestinal fluid; FeSSIF, fed-state simulated intestinal fluid; FaSSGF, fasted-state simulated gastric fluid; FNP, Flash NanoPrecipitation; GI, gastrointestinal; HPLC, high-performance liquid chromatography; MMV, Medicines for Malaria Venture; NP, nanoparticle; OA, sodium oleate; OZ FB, OZ439 free base; PBS, phosphate-buffered saline; PCL-PEG, polycaprolactone<sub>3,9kDa</sub>-*block*-poly(ethylene glycol)<sub>5kDa</sub>; PDI, polydispersity index; PS-PEG, poly(styrene)<sub>1.6kDa</sub>-*block*-poly(ethylene glycol)<sub>5kDa</sub>; SDS, sodium dodecyl sulfate; THF, tetrahydrofuran; WHO, World Health Organization

## REFERENCES

- (1) WHO, *World Malaria report, 2016*, <http://www.who.int/malaria/publications/world-malaria-report-2016/report/en/>.
- (2) Biamonte, M. A., Wanner, J., and Le Roch, K. G. (2013) Recent advances in malaria drug discovery. *Bioorg. Med. Chem. Lett.* 23 (10), 2829–2843.
- (3) Fairhurst, R. M., Nanyar, G. M. L., Breman, J. G., Hallett, R., Vennerstrom, J. L., Duong, S., Ringwald, P., Wellem, T. E., Plowe, C. V., and Dondorp, A. M. (2012) Artemisinin-Resistant Malaria: Research Challenges, Opportunities, and Public Health Implications. *Am. J. Trop. Med. Hyg.* 87 (2), 231–241.
- (4) Van Agtmael, M. A., Eggelte, T. A., and Van Boxtel, C. J. (1999) Artemisinin drugs in the treatment of malaria: from medicinal herb to registered medication. *Trends Pharmacol. Sci.* 20 (5), 199–205.
- (5) Bill & Melinda Gates Foundation, What We Do—Malaria, Strategy Overview, <http://www.gatesfoundation.org/What-We-Do/Global-Health/Malaria> (accessed Mar 16, 2017).
- (6) Sastry, S., Nyshadham, J., and Fix, J. (2000) Recent technological advances in oral drug delivery - a review. *Pharm. Sci. Technol. Today* 3 (4), 138–145.
- (7) Fasano, A. (1998) Novel approaches for oral delivery of macromolecules. *J. Pharm. Sci.* 87 (11), 1351–1356.

(8) Letchford, K., Liggins, R., and Burt, H. (2008) Solubilization of hydrophobic drugs by methoxy poly(ethylene glycol)-*block*-polycaprolactone diblock copolymer micelles: theoretical and experimental data and correlations. *J. Pharm. Sci.* 97 (3), 1179–1190.

(9) Robinson, J. R., and Lee, V. H. L. (1987) Influence of drug properties and routes of drug administration on the design of sustained and controlled release systems, *Controlled Drug Delivery: Fundamentals and Applications*, 2nd ed., CRC Press, Drugs and the Pharmaceutical Sciences 29, pp 3–61.

(10) Zhang, L., Gu, F. X., Chan, J. M., Wang, A. Z., Langer, R. S., and Farokhzad, O. C. (2008) Nanoparticles in medicine: therapeutic applications and developments. *Clin. Pharmacol. Ther.* 83 (5), 761–769.

(11) Peer, D., Karp, J. M., Hong, S., Farokhzad, O. C., Margalit, R., and Langer, R. (2007) Nanocarriers as an emerging platform for cancer therapy. *Nat. Nanotechnol.* 2 (12), 751–760.

(12) Budijono, S. J., Russ, B., Saad, W., Adamson, D. H., and Prud'homme, R. K. (2010) Block copolymer surface coverage on nanoparticles. *Colloids Surf., A* 360 (1–3), 105–110.

(13) Wu, L., Zhang, J., and Watanabe, W. (2011) Physical and chemical stability of drug nanoparticles. *Adv. Drug Delivery Rev.* 63 (6), 456–469.

(14) Cho, K., Wang, X., Nie, S., Chen, Z., and Shin, D. M. (2008) Therapeutic nanoparticles for drug delivery in cancer. *Clin. Cancer Res.* 14 (5), 1310–1316.

(15) Johnson, B. K., and Prud'homme, R. K. (2003) Flash NanoPrecipitation of Organic Actives and Block Copolymers using a Confined Impinging Jets Mixer. *Aust. J. Chem.* 56, 1021–1024.

(16) Johnson, B. K., and Prud'homme, R. K. (2003) Mechanism for Rapid Self-Assembly of Block Copolymer Nanoparticles. *Phys. Rev. Lett.* 91 (11), 118302.

(17) Saad, W. S., and Prud'homme, R. K. (2016) Principles of Nanoparticle Formation by Flash NanoPrecipitation. *Nano Today* 11 (2), 212–227.

(18) Johnson, B. K., and Prud'homme, R. K. (2003) Chemical processing and micromixing in confined impinging jets. *AIChE J.* 49 (9), 2264–2282.

(19) Charman, S. A., Arbe-Barnes, S., Bathurst, I. C., Brun, R., Campbell, M., Charman, W. N., Chiu, F. C. K., Chollet, J., Craft, J. C., Creek, D. J., Dong, Y., Matile, H., Maurer, M., Morizzi, J., Nguyen, T., Papastogiannidis, P., Scheurer, C., Shackelford, D. M., Sriraghavan, K., Stingelin, L., Tang, Y., Urwyler, H., Wang, X., White, K. L., Wittlin, S., Zhou, L., Vennerstrom, J. L., et al. (2011) Synthetic ozonide drug candidate OZ439 offers new hope for a single-dose cure of uncomplicated malaria. *Proc. Natl. Acad. Sci. U. S. A.* 108 (11), 4400–4405.

(20) Phyto, A. P., Jittamala, P., Nosten, F. H., Pukrittayakamee, S., Imwong, M., White, N. J., Duparc, S., Macintyre, F., Baker, M., and Möhrle, J. J. (2016) Antimalarial activity of artefenomel (OZ439), a novel synthetic antimalarial endoperoxide, in patients with Plasmodium falciparum and Plasmodium vivax malaria: an open-label phase 2 trial. *Lancet Infect. Dis.* 16, 61–69.

(21) Moehrle, J. J., Duparc, S., Siethoff, C., van Giersbergen, P. L. M., Craft, J. C., Arbe-Barnes, S., Charman, S. A., Gutierrez, M., Wittlin, S., and Vennerstrom, J. L. (2013) First-in-man safety and pharmacokinetics of synthetic ozonide OZ439 demonstrates an improved exposure profile relative to other peroxide antimalarials. *Br. J. Clin. Pharmacol.* 75 (2), 535–548.

(22) Rosenthal, P. J. (2016) Artefenomel: a promising new antimalarial drug. *Lancet Infect. Dis.* 16, 6–8.

(23) McCarthy, J. S., Baker, M., O'Rourke, P., Marquart, L., Griffin, P., Hooft van Huijsdijnen, R., and Möhrle, J. J. (2016) Efficacy of OZ439 (artefenomel) against early Plasmodium falciparum blood-stage malaria infection in healthy volunteers. *J. Antimicrob. Chemother.* 71, 2620–2627.

(24) Pinkerton, N., Grandeur, A., Fisch, A., Brozio, J., Riebeschl, B., and Prud'homme, R. (2013) Formation of stable nanocarriers by in situ ion pairing during block-copolymer-directed rapid precipitation. *Mol. Pharmaceutics* 10, 319–328.

- (25) He, Y., and Ho, C. (2015) Amorphous solid dispersions: utilization and challenges in drug discovery and development. *J. Pharm. Sci.* 104 (10), 3237–3258.
- (26) *Characterization of Nanoparticles Intended for Drug Delivery*, McNeil, S. E., Ed., Springer Protocols, 2011.
- (27) Biorelevant.com, FaSSGF, <https://biorelevant.com/fassif-fessif-fassgf/buy/> (accessed Apr 14, 2017).
- (28) ThermoFisher Scientific, PBS, pH 7.4, <https://www.thermofisher.com/order/catalog/product/10010023> (accessed Apr 14, 2017).
- (29) Owens, D. E., III, and Peppas, N. A. (2006) Opsonization, biodistribution, and pharmacokinetics of polymeric nanoparticles. *Int. J. Pharm.* 307 (1), 93–102.
- (30) Dow Chemicals, 2013, DOI: 10.1021/acsinfecdis.7b00278.
- (31) Abdelwahed, W., Degobert, G., Stainmesse, S., and Fessi, H. (2006) Freeze-drying of nanoparticles: formulation, process and storage considerations. *Adv. Drug Delivery Rev.* 58 (15), 1688–1713.
- (32) Le, J., Drug Absorption, <http://www.merckmanuals.com/professional/clinical-pharmacology/pharmacokinetics/drug-absorption>.
- (33) Malvern, 2011.
- (34) Malvern Instruments Ltd, *Zetasizer Nano Series User Manual*, pp 1–12.
- (35) Speakman, S. A., Basics of X-Ray Powder Diffraction, <http://prism.mit.edu/xray/oldsite/1%20Basics%20of%20X-Ray%20Powder%20Diffraction.pdf>
- (36) Royal Society of Chemistry, Chemspider, <http://www.chemspider.com/> (accessed Apr 25, 2017).
- (37) ACE. ACE and JChem acidity and basicity calculator, <https://ace.chem.illinois.edu/ace/> (accessed Apr 25, 2017).
- (38) Molinspiration, Calculation of Molecular Properties, <http://www.molinspiration.com/cgi-bin/properties> (accessed Apr 25, 2017).
- (39) Zhang, Y., Feng, J., McManus, S. A., et al. (2017) Design and Solidification of Fast-Releasing Clofazimine Nanoparticles for Treatment of Cryptosporidiosis. *Mol. Pharmaceutics* 14 (10), 3480–3488.
- (40) Lu, H., Rummaneethorn, P., Ristroph, K. D., and Prud'homme, R. K. (2018) Hydrophobic Ion Pairing of Peptide Antibiotics for Processing into Controlled Release Nanocarrier Formulations. *Mol. Pharmaceutics* 15 (1), 216–225.